Minerals **2014**, *4*, 565-577; doi:10.3390/min4030565

OPEN ACCESS

minerals

ISSN 2075-163X
www.mdpi.com/journal/minerals

Article

Silicon-Rich, Iron Oxide Microtubular Sheath Produced by an Iron-Oxidizing Bacterium, *Leptothrix* sp. Strain OUMS1, in Culture

Hiromichi Ishihara [1], Hideki Hashimoto [1], Eisuke Taketa [1], Tomoko Suzuki [1], Kyoko Mandai [1], Hitoshi Kunoh [1] and Jun Takada [1,2,*]

[1] Graduate School of Natural Science and Technology, Okayama University, Okayama 700-8530, Japan; E-Mails: hishihara@cc.okayama-u.ac.jp (H.I.); hideki-h@cc.okayama-u.ac.jp (H.H.); en421232@s.okayama-u.ac.jp (E.T.); suzukito@cc.okayama-u.ac.jp (T.S.); mandai-k@cc.okayama-u.ac.jp (K.M.); hkunoh@cc.okayama-u.ac.jp (H.K.)

[2] Core Research for Evolutionary Science and Technology (CREST), Japan Science and Technology Agency (JST), Okayama 700-8530, Japan

* Author to whom correspondence should be addressed; E-Mail: jtakada@cc.okayama-u.ac.jp; Tel.: +81-86-251-8107; Fax: +81-86-251-8087.

Received: 11 April 2014; in revised form: 3 June 2014 / Accepted: 23 June 2014 / Published: 27 June 2014

Abstract: This study aimed to manipulate the texture and elemental composition of the novel sheaths produced by the iron-oxidizing bacterium *Leptothrix* in culture by altering components of the medium. When previously isolated strain OUMS1 was cultured in media (pH 7.0 throughout incubation) containing various levels of Si on a rotary shaker at 20 °C and 70 rpm for 14 days, the strain was able to reproduce in media with up to 300 ppm Si, and the hollow microtubular architecture of the sheath was maintained even at 300 ppm Si. The constitutional iron oxide phase changed from poorly crystalline lepidocrocite at 0 ppm Si to X-ray diffraction (XRD)-amorphous 2-line ferrihydrite at 100–300 ppm via their mixture phase with intermediate Si content (Si-30 and -50 ppm). The results strongly indicate that the chemical character and crystallinity of the sheath texture can be regulated by culture conditions, especially components of the medium.

Keywords: *Leptothrix* sp. strain OUMS1; sheath formation; iron oxide; silicon-rich sheath; phase change of iron oxides

---

1. Introduction

Some bacteria serve as distinct nucleation sites for mineral authigenesis *in situ* [1]. Such processes of iron (Fe) and manganese (Mn) deposition in terrestrial and aquatic habitats are often attributed to microbial activity [2]. A restricted number of aquatic bacterial species, mainly those belonging to the genera *Sphaerotilus* and *Leptothrix*, form extracellular microtubular sheaths with an X-ray diffraction (XRD)-amorphous texture composed of organic bacterial secretions and aquatic inorganics such as Fe, silicon (Si), phosphorus (P), and often calcium (Ca). The mechanism of this type of sheath formation is closely associated with the capacity of these organisms to accumulate and oxidize Fe and Mn in aquatic environments [3,4]. Thus far, a body of evidence and several hypotheses related to architecture and chemical and physical characters of the sheath have been summarized and discussed in a number of reviews [1,3–6].

Characteristic traits that distinguish members of the genera *Leptothrix* and *Sphaerotilus* from other phylogenetically related species are the ability to form tubular sheaths and to precipitate copious amounts of oxidized iron or manganese [7]. Sawayama *et al.* [8] who first isolated OUMS1 reported that this strain produced clusters of hollow microtubular sheaths on the iron plates when cultured in SIGP (Silicon-Iron-Glucose-Peptone) liquid medium (hereafter referred to as cultured sheaths). Furutani *et al.* [9] confirmed by electron microscopy that the outer coat of the cultured sheaths was composed of loosely woven thin fibrils and that the entire wall of the sheath was 0.3–0.4 μm thick.

Recently, Hashimoto *et al.* [10] proposed a structural model for the iron oxides produced by *Leptothrix ochracea* in which the XRD-amorphous structure of the basic texture of the sheath is constructed of an FeO_6 network intermingled with SiO_4, suggesting that Si could be a key unit of the XRD-amorphous structure. Sawayama *et al.* [8] isolated *Leptothrix* sp. strain OUMS1 (hereafter, simply OUMS1) and devised a silicon-iron-glucose-peptone medium (hereafter referred to as SIGP) for its cultivation. Our previous electron microscopic and spectroscopic studies proved that the sheath was an ingenious hybrid of organic and inorganic materials resulting from the interaction between bacterial exopolymers and aqueous-phase inorganics such as Fe, P, and Si in aquatic environments [9,11,12]. Earlier studies [13–16] concerning biomineralization by Fe-oxidizing bacteria led us to consider that interactions between the bacterial organics and aqueous-phase inorganics were probably mediated by inorganic processes rather than by the organic chemistry of the stalk or sheath. Chan *et al.* [13] considered that the carboxyl groups of the polysaccharides released from the bacterial cells could play an important role in the *Mariprofundus* biomineralization. Although these studies provided further insights into the structural and spatial associations among the constitutional elements in the sheath of Fe-oxidizing bacteria including *Leptothrix*, more information is needed to understand the initiation and construction of such unique hybrid structures. Suzuki *et al.* [17] compared the morphological features of sheaths produced by OUMS1 in a culture medium with those formed in natural groundwater conditions and found that sheaths in culture had a thicker wall covered with thicker fibrils than those in the groundwater. Their results led us to assume that we might be able to regulate the composition of the sheath texture by modifying the amount of the inorganic elements in the medium. To verify this assumption, we prepared modified media that contained various concentrations of sodium silicate in a study focused on the structural and compositional differences between strain OUMS1 grown in an SIGP and the modified Si-rich media. This study aimed to create new functional materials by culturing

OUMS1, because natural *Leptothrix* sheaths have been noted to have a variety of industrial applications such as a lithium ion battery electrode material [18], a catalyst enhancer [19–21], and a pottery pigment [22]. Controlling the composition of the sheaths would further increase the usefulness of the material. This study aimed to create new functional materials by culturing OUMS1. We used scanning transmission electron microscopy (STEM), high-angle annular dark field (HAADF)-STEM imaging, scanning electron microscopy (SEM), energy dispersive X-ray (EDX) spectroscopy, and powder X-ray diffractometry (XRD) to qualitatively and quantitatively analyze subsequent sheath formation in the modified media.

2. Experimental Section

2.1. Culture Conditions

Initially, we confirmed that when OUMS1 was cultured in the basic silicon-glucose-peptone (SGP) medium [8] (glucose,1 g; Bacto peptone (Becton, Dickinson and Company, Franklin Lakes, NJ, USA), 1 g; $Na_2SiO_3 \cdot 9H_2O$, 0.2 g; $CaCl_2 \cdot 2H_2O$, 0.044 g; $MgSO_4 \cdot 7H_2O$, 0.041 g; $Na_2HPO_4 \cdot 12H_2O$, 0.076 g; $KH_2PO_4 \cdot 2H_2O$, 0.02 g; HEPES, 2.838 g in 1000 mL of filter-sterilized (0.22 μm pore size Millipore (Billerica, MA, USA)) water (the final pH was adjusted to 7.0 with 0.1 N NaOH after the components were mixed)), a cluster of sheaths formed on the Fe plates and that their morphology was consistent with that reported previously [9,11,17]. We monitored pH in the flasks every day during incubation and found that the pH values remained 6.6–7.3 (6.8–7.1 most days) for 14 days (mean values of triplicate each day).

The basic SGP medium contained 19.8 ppm of Si and 10.2 ppm of the P components. Because 2 ppm of the P components was confirmed to be enough to maintain the bacterial reproduction, the concentration of P components added to media was fixed at 2 ppm in this study. Because Si precipitated as white substance in media with more than 300 ppm Si (equivalent to 10.68 mM of sodium silicate), we used 0 to 300 ppm Si content in the media. When we tested these concentrations of sodium silicate for their effect on reproduction at 1 week after incubation, the mean number of cfu/mL was estimated as 3.3×10^6 cfu/mL in 0 ppm, 2.2×10^6 cfu/mL in 30 ppm Si (1.068 mM of sodium silicate), 2.5×10^6 cfu/mL in 300 ppm Si, indicating that the cells survived in the presence of a high amount of sodium silicate.

These preliminary results led us to focus on sheath formation in media containing 0, 11.5 (0.4095 mM of sodium silicate), 30 (1.068 mM), 50 (1.780 mM), 100 (3.561 mM), and 300 ppm of Si. In the results described in detail next, we used abbreviations Si-0 to Si-300 for these media.

According to the protocols of Sawayama *et al.* [8] and Suzuki *et al.* [17], OUMS1 (NITE BP-860) was cultured in liquid media. We used a silicon-glucose-peptone (SGP) liquid medium with three iron (Fe) plates ($10 \times 10 \times 1.2$ mm^3; 99.9% purity; Kojundo Chem. Lab., Saitama, Japan) but no $FeSO_4$ (hereafter referred to as basic SGP, *i.e.*, original SIGP minus $FeSO_4$). The Fe plates remained almost stable on the culture flask during the rotation culture. Holding the P component constant at 2 ppm and using the three Fe plates in 100 mL culture medium, we modified the concentration of sodium silicate (stock solution: 35.61 mM equivalent to 1000 ppm Si) in the basic SGP to fit our experimental purpose. The initial bacterial inoculum density was 1.0×10^1 cfu/mL. The respective inoculated media

with varied concentrations of sodium silicate were separately incubated on a rotary shaker at 20 °C and 70 rpm for 14 days. Samples were scraped from Fe plates and repeatedly washed with sterilized ultrapure water for less than one minute and freeze-dried to use for the experiments.

The number of viable OUMS1 cells in the media was estimated by dilution plating method as described by Suzuki *et al.* [17]. The 1-week-cultured bacterial suspension was serially diluted and spotted onto basic SGP agar plates. After 3 days of incubation at 20 °C, colonies on the plates were counted with a stereomicroscope, and the population was expressed as cfu/mL.

2.2. Transmission Electron Microscopy (TEM) Measurements

Dried specimens were also resuspended in 100% ethanol, mounted onto Cu grids precoated with an amorphous lacy carbon film, and air-dried for HAADF-STEM and transmission electron microscopy (TEM). HAADF-STEM and EDX detectors attached to the microscope (JEM-2100F (JEOL, Tokyo, Japan), accelerating voltage: 200 kV) were used for HAADF-STEM imaging and elemental mapping of Si, Fe, O, and P in samples, respectively. Electron diffraction (ED) and fast Fourier transform (FFT) patterns of the sheath matrix were obtained during the TEM observation. Ten fibers stretching from the outer sheath surface in STEM images were measured to obtain a mean fiber width.

2.3. Qualitative and Quantitative Energy Dispersive X-Ray (EDX) Analysis of Si, Fe, O, and P in Sheaths

A suspension of the washed specimens was dropped onto a carbon tape on an aluminum stub and vacuum-dried to analyze the elemental composition of samples using an energy dispersive X-ray microanalyzer attached to a scanning electron microscope (SEM-EDX) (S-4300, Hitachi, Tokyo, Japan). For qualitative analysis, a distribution map of the inorganic elements in randomly selected sheaths was obtained. For quantitative analysis, the composition ratio (atomic %) was obtained at different views and magnifications for at least five sheaths. Mean ratios and standard deviations are shown in Figure 3B.

2.4. X-Ray Diffractometry (XRD) Measurements

X-ray diffraction patterns were obtained using an RINT-2000 (Rigaku, Tokyo, Japan) with Cu-Kα radiation (voltage, 40 kV; current, 200 mA). The dried samples were pressed into an XRD holder with a glass plate to flatten the surface of the compacted powders. Scans were performed from 10°–38.8° and 44°–80° (2θ value) with a step size of 0.02° at a fixed time of 1 s. The XRD pattern of XRD holder was measured and the pattern was subtracted from samples' XRD pattern.

3. Results and Discussion

3.1. Morphology, Size and Electron Diffraction (ED)-Results of Sheaths

When OUMS1 was cultured in Si-0, microtubular sheaths covered with fibers were formed (Figure 1a). The HAADF-STEM image of the same structure showed that the sheath looked hollow and had a 50–100-nm-thick wall covered with hairy fibers (Figure 1d). In an enlarged image of the outer surface

of the same sheath (Figure 2a), the outer fibers were composed of agglutinated fibrils and thin films. A highly magnified image of TEM showed that the ethanol-insoluble texture of the outer surface was a very thin, tabular structure (Figure 2f) of homogeneous-looking fine particles. The tabular structures looked like crumpled sheets, with wrinkled patterns in the texture. The ED pattern acquired from the texture (Figure 2f, inset) indicates that the major component of the texture is a poorly crystalline lepidocrocite, γ-FeOOH. In the Si-11.5 medium, a similar microtubular structure was covered with agglutinated fibrils in a texture (Figure 2b) that had a similar ED pattern (data not shown). The sheaths in Si-30 to -300 also had the typical hollow microtubular shape (Figure 1b,c), but the FFT pattern showed that the texture had changed to the XRD-amorphous state in Si-30 and -300 (Figure 2g,h, inset). Although these microtubules were covered with a layer of agglutinated fibrils, the structure was thicker as the amount of Si increased in the medium: its average thickness was *ca*. 4 nm in Si-30, 9 nm in Si-50, 16 nm in Si-100, and 39 nm in Si-300 (Figure 2c–e). These thicker fibers were probably formed by agglutination of more fibrils and/or more extracellular organic secretions from the bacterial cells, which served as a glue. Enlarged TEM images of the sheaths in Si-30 and Si-300 illustrate nanoparticles with a diameter of *ca*. 5 nm (Figure 2g,h), differing from those formed in Si-0 and Si-11.5. FFT images showed a halo pattern in the outer surface texture of the sheaths in Si-30 to Si-300 (Figure 2g,h, inset), indicating FFT-amorphous ionic arrangements with poor medium- to long-range ordering.

Figure 1. Scanning transmission electron microscopy (STEM) images of cultured sheaths having different Si composition ratios. Secondary electron images ((**a**) Si-0, (**b**) Si-30, (**c**) Si-300)) and high-angle annular dark field (HAADF) images ((**d**) Si-0, (**e**) Si-30, (**f**) Si-300)) showing hollow microtubular structures of which surface was covered with hairy fibers at all concentrations of Si used in the media.

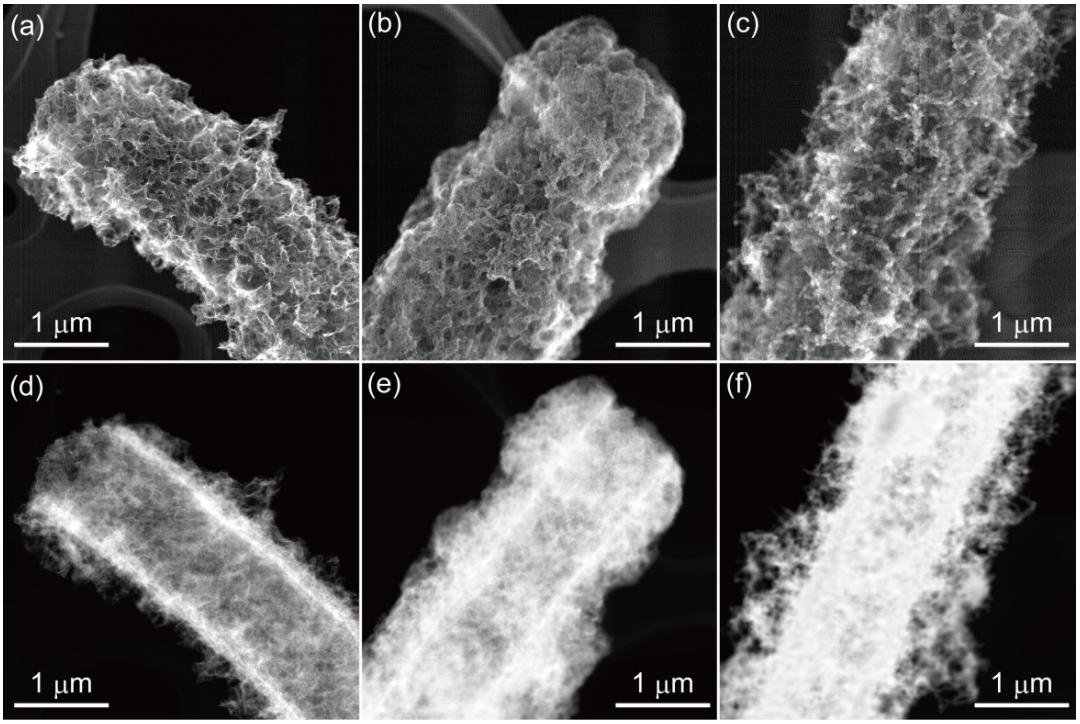

Figure 2. STEM and transmission electron microscopy (TEM) images of fibers covering the respective cultured sheath surfaces. Secondary electron images of outer surface texture of ((**a**) Si-0, (**b**) Si-11.5, (**c**) Si-30, (**d**) Si-50, and (**e**) Si-300. TEM images of outer surface texture of (**f**) Si-0, (**g**) Si-30, and (**h**) Si-300. Note the crumpled sheets in the texture of Si-0 and the nanoparticles (circled) comprising the texture of Si-30 and -300. Inset: (**f**) electron diffraction (ED) pattern and (**g**,**h**) fast Fourier transform (FFT) pattern.

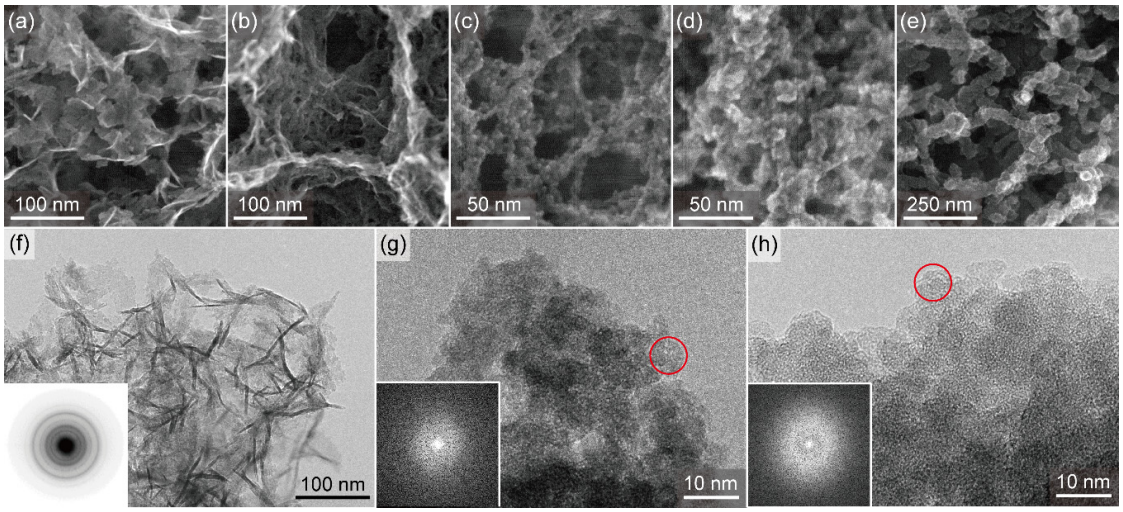

Ghiorse [4] noted that the forms of sheaths produced by iron-oxidizing bacteria can change under different cultural conditions. Rogers and Anderson [23] investigated physiology of Fe deposition of an Fe-precipitating strain of *Sphaerotilus* in laboratory culture with different Fe concentrations in media to characterize the process, and reported that the growth rate was apparently independent of the Fe concentration in media and that Fe deposition could be mediated by certain of the constituents of the organism's sheath. Additionally they emphasized that the system that mediated Fe deposition appeared to be self-sustaining after certain cellular (sheath) constituents had been synthesized, and the deposition was triggered at the end of the exponential growth phase of the bacterium. Interestingly, in our study, regardless of the level of Si in the medium, the basic hollow, microtubular construct was similar to that of the sheath produced in the original SIGP medium [9,11,17], even at the highest level tested (Si-300). In a previous paper [9], we reported that basic sheath construction by OUMS1 proceeded in two steps under culture conditions: an initial assembly of saccharic bacterial fibrils that originated from the cell envelope, then the aqueous-phase deposition of Fe, P, and Si. These results suggest that organic materials released from the cells might form the initial frame of sheaths enough to trigger the element deposition, regardless of Si concentrations in media, as similarly as those of *Sphaerotilus* [23].

3.2. Elemental Analysis and Ratios of Sheaths

Although an elevated level of Si in the media did not drastically affect the basic architecture of the sheath and bacterial cell reproduction, the microscopy results suggested that the phase of the sheath texture might be affected by the concentration of sodium silicate in the medium. Hence, we quantitatively and qualitatively analyzed the elemental composition of the sheath texture produced under varied amounts of Si in media.

With the EDX analysis, we detected Fe, Si, and O distributed nearly uniformly in the sheaths and their outer, "hairy" structures, regardless of the concentration of Si (Si-0 to Si-300) (Figure 3b–d). Because all the media contained the same low amount of P, the distribution of P did not clearly differ in any of the sheaths (Figure 3e). The nearly uniform distribution of elements was very similar to that in sheaths produced in the original SIGP medium except for the P distribution [9]. Figure 3B shows the elemental ratios (atomic %) in sheaths produced in media with different Si levels. As expected, the ratio of Fe was extremely high, and those of Si and P were quite low in Si-0 medium: Fe:Si:P = 95:2:3. The ratio of Fe in sheaths decreased gradually as the Si level increased in media and reached *ca*. 50 atomic % in Si-300. By contrast, the ratio of Si in sheaths gradually increased with increasing amounts of Si in the media and reached the maximum of *ca*. 50 atomic % in Si-300. The average ratio of Fe:Si:P in sheaths produced in various media was 87:11:2 in Si-11.5, 76:21:3 in Si-30, 68:31:1 in Si-50, 57:41:1 in Si-100, and 50:49:1 in Si-300. As indicated by these ratios, atomic % of P ranged from 1% to about 3% irrespective of the amount of Si in the medium, probably due to the presence of the low amount of the P component always present. The relatively small standard deviations of average atomic % (Figure 3B) reflect the uniform distribution of these elements in sheaths. The sheaths produced by OUMS1 in culture were reported to have a mean Si content of less than 20 atomic % [8], similar to those produced by *Leptothrix* species in natural environments [12,24]. High concentrations of Si in media probably influence secretion of saccharic fibrils in the first step of sheath formation, resulting in thicker fibers, because cell reproduction was similar in Si-0–300, as described earlier. According to these data, we should be able to vary the amount of Si in the medium to manipulate the bacteria to create sheaths with a quantitative balance of Fe and Si that is desired for industrial purposes.

Figure 3. (**A**) Elemental mapping of the cultured sheath of Si-300 (Fe:Si:P = 50:49:1) obtained by energy dispersive X-ray (EDX) area analysis. (**a**) HAADF-STEM image of a microtubule produced in Si-300. (**b**–**e**) Distribution maps of Fe, Si, O, and P, respectively, in the view area of (**a**). (**B**) Average ratios of Fe, Si, and P in the sheaths in media with various amounts of Si. Fe: black triangle, Si: blue circle, P: red square.

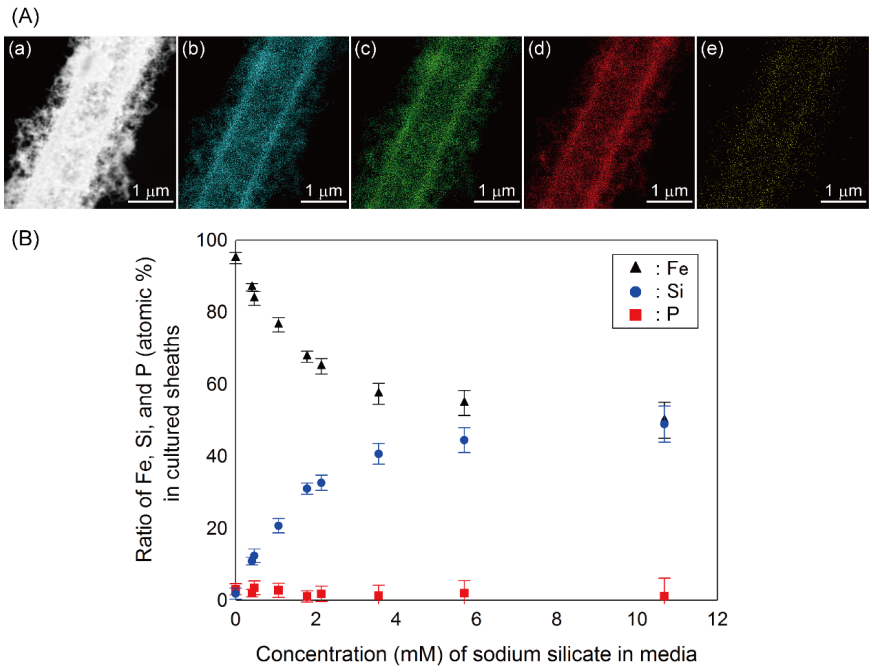

3.3. ED/XRD-Results and Crystallinity of Sheaths

On the basis of the ED and FFT patterns (Figure 2), the texture of the sheaths seemed to be affected by the amount of Si in the medium. According to the XRD patterns (Figure 4), the cultured sheaths in Si-0 and Si-11.5 had major diffraction peaks at 2θ = 27°, 36.3°, 46.9°, and 60.4°, which corresponds to those of lepidocrocite (ICDD database, PDF 00-044-1415; Figure 4a,b, black circles). Cornell and Schwertmann [25] noted that the crystal habit of lepidocrocite varied with the conditions under which oxidation of Fe^{2+} took place and that rapidly precipitated lepidocrocite grew as thin, crumpled sheets. Thus, the crumpling feature of Si-0 in Figure 2f suggests that the lepidocrocite forms rapidly under the present cultivation conditions in Si-0 and -11.5. Similar to a finding by Eggleton *et al.* [26], we observed a very broad peak at 30°–40° (black triangle), which plausibly was derived from 2-line ferrihydrite (2Fh), for Si-11.5 to Si-300. Based on these patterns, the sheath texture in Si-0 and -11.5 was composed of a single phase of poorly crystalline lepidocrocite and a mixed phase of 2Fh and poorly crystalline lepidocrocite, respectively. Decreased peak intensity and broadened peak width of lepidocrocite with increasing Si content up to 30 ppm in media probably reflect decrease of crystallinity and/or particle size. In Si-30 to Si-300, the broad peak at 30°–40° was even broader probably due to an enhanced amount of 2Fh, leading to lower crystallinity of the texture. It is likely that 2Fh was the main phase in Si-30 and Si-50, but the slight peak of lepidocrocite was detected in the vicinity of 60°, suggesting that the Si-30 and Si-50 texture might be composed of a small amount of lepidocrocite with a large amount of 2Fh. In Si-50, only the broad peaks of 2Fh were observed. This observation was in accordance with the earlier report by Châtellier *et al.* [27] that large quantities of aqueous silica favored the formation of 2Fh in the presence of various bacterial cells. A bulge derived from XRD-amorphous silica in the vicinity of 24° (black square) was distinguished, especially for Si-100 and Si-300. The results suggest that the texture in Si-100 and Si-300 could comprise a large amount of 2Fh and a small amount of XRD-amorphous silica. Karim [28] reported a similar phase change of Fe oxides by oxidation of $FeCl_2$ solution containing different amounts of silica: lepidocrocite was formed in the solution having initial atomic Si/Fe ratio = 0, well-crystalized ferrihydrite/some feroxylite/trace lepidocrocite + goethite at Si/Fe ratio=18.0×10^{-3} and poorly crystallized ferryhydrite at Si/Fe ratio > 35.6×10^{-3}. Although Carlson and Schwertmann [29] noted that Si-O-Fe bonds were probably responsible for stability of natural ferrihydrite which always contained some silica, the role of Si in Fe/Si complex in abiotic system has not been well understood. Because the crystallinity of synthetic 2Fh is lowered when the structure is doped with Si [30–32], the Si-dependent changes of the texture found in the present study may not directly be associated with the existence of OUMS1, but result from direct autocatalytic oxidation, chemical/physical interactions, among elements. Referring the earlier paper [33] that organics were responsible for the poor crystallinity of microbe-associated Fe minerals, the crystallinity change observed in this study could be dependent on not only Si but also the bacterial organics. To verify this hypothesis, we need to determine how Si interacts with the Fe complex in the texture and how the organic material from the bacteria interacts with aqueous-phase elements.

Figure 4. X-ray diffractometery (XRD) patterns of cultured sheaths in media with different Si contents. (**a**) Si-0, (**b**) Si-11.5, (**c**) Si-30, (**d**) Si-50, (**e**) Si-100, and (**f**) Si-300. The positions of the diffraction peaks were assigned using the ICDD database. The main diffraction peak for lepidocrocite (black circle), 2Fh (black triangle), and XRD-amorphous silica (black square) is indicated. The position of the diffraction peaks in ICDD database of lepidocrocite (PDF 00-044-1415) and in reference 16 of 2Fh are given as black and red bars in the bottom of the figure, respectively. The break near 40° corresponds to the peaks derived from the sample holder.

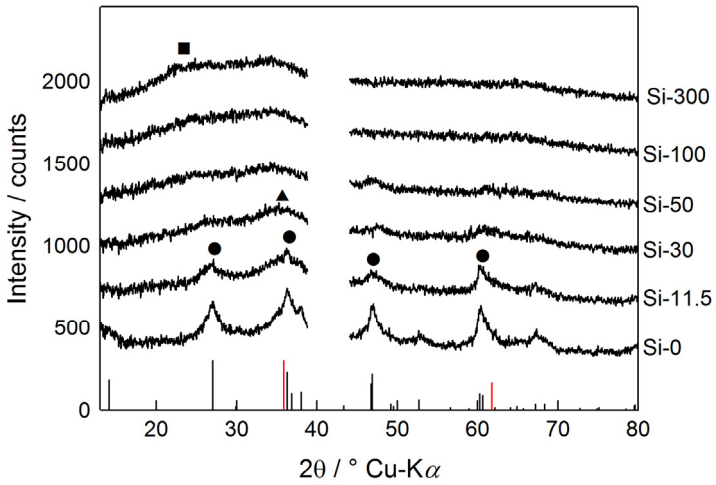

Leptothrix species deposit copious amounts of iron hydroxide-encrusted sheaths in the environment where they grow [4]. Chemically active saccharic and proteinaceous groups in the secretions of bacteria are thought to play a key role in binding aqueous inorganic ions [4,9,11,12,34–37]. Although Hashimoto *et al.* [18] found a variety of chemical bonds such as Fe–O, Fe–O–Si, Fe–O–P and so on in *Leptothrix* sheaths, it is still unknown how these chemical bonds are formed in the sheaths: are the iron hydroxides and oxides formed first, then other ions bind to them or *vice versa*? The present finding that the microtubular form of sheaths was maintained even in Si-0 and Si-300 suggests that the form itself is not associated with the balance of Fe and Si in the sheaths. However, the outer fibers of the sheaths were primarily affected by the amount of Si. The outer thick fibers in Si-30 and Si-300, which were probably caused by agglutination of fine fibrils secreted from bacterial cells, suggest that elevated amounts of sodium silicate in the medium might affect the secretion by bacterial cells, because the organic secretion is thought to glue the fine fibrils together to form a thick fibrous core of the sheath architecture [9]. Because the organic texture formed by biomineralization, in most cases, a complex assemblage of polysaccharides and proteins, is considered to be associated with mineral nucleation [13], the control of the location and organization of nucleation sites, the structure and crystallographic orientation of the inorganic phase [38], and the interaction of the organic texture and aqueous phase of inorganics are target issues to be studied in the presence of large quantity of Si.

As mentioned already, the sheath material of *Leptothrix* has a variety of attractive functions for industrial purposes [18–22,39,40]. We expect that the biologically created Si-rich sheaths will have additional functions that will be useful as an industrial material. We are currently investigating novel functions for the Si-rich sheaths using various approaches, and these studies will be the subject of forthcoming publications by this group.

4. Conclusions

An isolated strain of *Leptothrix* sp., OUMS1, was cultivated in media containing different concentrations of sodium silicate. The composition ratio of inorganic elements and detailed morphological architecture of the sheaths produced during cultivation were analyzed mainly by electron microscopy. Results demonstrated that (i) the hollow, microtubular architecture was maintained in media containing Si up to 300 ppm, although the outer fibrous feature changed with elevated concentrations of Si; (ii) with increasing amounts of Si in the medium, the Fe-related phase composing the basic texture of the sheath changed from poorly crystalline lepidocrocite to XRD-amorphous 2Fh and changed their mixture phase with elevated Si levels in the medium; (iii) Fe content in sheaths decreased, but Si content increased when Si content was elevated. Thus, the use of media with different compositions was very efficient for fabricating sheath materials having unprecedented chemical textures and is expected to have industrial applications as novel functional materials.

Acknowledgments

We express our sincere appreciation to our colleagues Daisuke Nakatsuka, Tsuyoshi Maeda, and Keiko Toyoda for their technical support through this study. We also acknowledge B. E. Hazen for reviewing and editing the manuscript. This study was financially supported by the Special Grant for Education and Research (2008–2013) from the Ministry of Education, Culture, Sports, Science, and Technology, Japan (Jun Takada) and Japan Society for the Promotion of Science, Grant-in-Aid for Young Scientists (B), Grant Number 24780073 (Tomoko Suzuki).

Author Contributions

Hiromichi Ishihara designed the overall experimental concept. Hideki Hashimoto conducted the electron microscopic analysis. Eisuke Taketa completed the XRD analysis. Tomoko Suzuki and Kyoko Mandai provided expertise to the microbiological cultivation. Hitoshi Kunoh and Jun Takada had original concept for the project. All authors participated in writing of the manuscript.

Conflicts of Interest

The authors declare no conflict of interest.

References

1. Ferris, F.G.; Fyfe, W.S.; Beveridge, T.J. Bacteria as nucleation sites for authigenic minerals in a metal-contaminated lake sediment. *Chem. Geol.* **1987**, *63*, 225–232.
2. Ghiorse, W.C.; Hirsch, P. An ultrastructural study of iron and manganese deposition associated with extracellular polymers of pedomicrobium-like budding bacteria. *Arch. Microbiol.* **1979**, *123*, 213–226.
3. Van Veen, W.L.; Mulder, E.G.; Deinema, M.H. The *Sphaerotilus-Leptothrix* group of bacteria. *Microbiol. Rev.* **1978**, *42*, 329–356.

4. Ghiorse, W.C. Biology of iron- and manganese-depositing bacteria. *Annu. Rev. Microbiol.* **1984**, *38*, 515–550.
5. Emerson, D.; Fleming, E.J.; McBeth, J.M. Iron-oxidizing bacteria: An environmental and genomic perspective. *Annu. Rev. Microbiol.* **2010**, *64*, 561–583.
6. Fleming, E.J.; Langdon, A.E.; Martinez-Garcia, M.; Stepanauskas, R.; Poulton, N.J.; Masland, E.D.P.; Emerson, D. What's new is old: Resolving the identity of *Leptothrix ochracea* using single cell genomics, pyrosequencing and FISH. *PLoS One* **2011**, *6*, 1–16.
7. Spring, S. The genera *Leptothrix and Sphaerotilus*. *Prokaryotes* **2006**, *5*, 758–777.
8. Sawayama, M.; Suzuki, T.; Hashimoto, H.; Kasai, T.; Furutani, M.; Miyata, N.; Kunoh, H.; Takada, J. Isolation of a *Leptothrix* strain, OUMS1, from ocherous deposits in groundwater. *Curr. Microbiol.* **2011**, *63*, 173–180.
9. Furutani, M.; Suzuki, T.; Ishihara, H.; Hashimoto, H.; Kunoh, H.; Takada, J. Initial assemblage of bacterial saccharic fibrils and element deposition to form an immature sheath in cultured *Leptothrix* sp. strain OUMS1. *Minerals* **2011**, *1*, 157–166.
10. Hashimoto, H.; Fujii, T.; Kohara, S.; Asaoka, H.; Kusano, Y.; Ikeda, Y.; Nakanishi, M.; Benino, Y.; Nanba, T.; Takada, J. Amorphous structure of iron oxide of bacterial origin. *Mater. Chem. Phys.* **2012**, *137*, 571–575.
11. Furutani, M.; Suzuki, T.; Ishihara, H.; Hashimoto, H.; Kunoh, H.; Takada, J. Assemblage of bacterial saccharic microfibrils in sheath skeleton formed by cultured *Leptothrix* sp. strain OUMS1. *J. Mar. Sci. Res. Dev.* **2011**, *5*, doi:10.4172/2155-9910.S5-001.
12. Suzuki, T.; Hashimoto, H.; Ishihara, H.; Kasai, T.; Kunoh, H.; Takada, J. Structural and spatial associations between Fe, O, and C in the network structure of the *Leptothrix ochracea* sheath surface. *Appl. Environ. Microbiol.* **2011**, *77*, 7873–7875.
13. Chan, S.C.; Fakra, S.C.; Emerson, D.; Fleming, E.J.; Edwards, K.J. Lithotrophic iron-oxidizing bacteria produce organic stalks to control mineral growth: Implications for biosignature formation. *ISME J.* **2011**, *5*, 717–727.
14. Ferris, F.G.; Schultze, S.; Witten, T.C.; Fyfe, W.S.; Beveridge, T.J. Metal interactions with microbial biofilms in acidic and neutral pH environments. *Appl. Environ. Microbiol.* **1989**, *55*, 1249–1257.
15. Hallberg, R.; Ferris, F.G. Biomineralization by *Gallionella*. *Geomicrobiol. J.* **2004**, *21*, 325–330.
16. Kennedy, C.B.; Scott, S.D.; Ferris, F.G. Characterization of bacteriogenic iron oxide deposits from axial volcano, Juan de Fuca Ridge, Northeast Pacific Ocean. *Geomicrobiol. J.* **2003**, *20*, 199–214.
17. Suzuki, T.; Ishihara, H.; Furutani, M.; Shiraishi, T.; Kunoh, H.; Takada, J. A novel method for culturing of *Leptothrix* sp. strain OUMS1 in natural conditions. *Minerals* **2012**, *2*, 118–128.
18. Hashimoto, H.; Hashimoto, H.; Kobayashi, G.; Sakuma, R.; Fujii, T.; Hayashi, N.; Kanno, R.; Takano, M.; Takada, J. Bacterial nanometric amorphous Fe-based oxide: A potential lithium-ion battery anode material. *ACS Appl. Mater. Interfaces* **2014**, *6*, 5374–5378.
19. Ema, T.; Miyazaki, Y.; Kozuki, I.; Sakai, T.; Hashimoto, H.; Takada, J. Highly active lipase immobilized on biogenous iron oxide via an organic bridging group: The dramatic effect of the immobilization support on enzymatic function. *Green Chem.* **2011**, *13*, 3187–3195.

20. Ema T.; Miyazaki, Y.; Taniguchi, T.; Takada, J. Robust porphyrin catalysts immobilized on biogenous iron oxide for the repetitive conversions of epoxides and CO_2 into cyclic carbonates. *Green Chem.* **2013**, *15*, 2485–2492.
21. Mandai, K.; Korenaga, T.; Ema, T.; Sakai, T.; Furutani, M.; Hashimoto, H.; Takada, J. Biogenous iron oxide-immobilized palladium catalyst for the solvent-free Suzuki–Miyaura coupling reaction. *Tetrahedron Lett.* **2012**, *53*, 329–332.
22. Hashimoto, H.; Asaoka, H.; Nakano, T.; Kusano, Y.; Ishihara, H.; Ikeda, Y.; Nakanishi, M.; Fujii, T.; Yokoyama, T.; Horiishi, N.; Nanba, T.; Takada, J. Preparation, microstructue, and color tone of microtubule material composed of hematite/amorphous-silicate nonocomposite from iron oxide of bacterial origin. *Dye. Pigment.* **2012**, *95*, 639–643.
23. Rogers, S.R.; Anderson, J.J. Measurement of growth and iron deposition in *Sphaerotilus discophorus*. *J. Bacteriol.* **1976**, *126*, 257–263.
24. Hashimoto, H.; Yokoyama, S.; Asaoka, H.; Kusano, Y.; Ikeda, Y.; Seno, M.; Takada, J.; Fujii, T.; Nakanishi, M.; Murakami, R. Characteristics of hollow microtubes consisting of amorphous iron oxide nanoparticles produced by iron oxidizing bacteria, *Leptothrix ochracea*. *J. Magn. Magn. Mater.* **2007**, *310*, 2405–2407.
25. Schwertmann, U.; Cornell, R.M. *Iron Oxides in the Laboratory: Preparation and Characterization*, 2nd ed.; Wiley-VCH: Weinheim, Germany, 2000; pp. 154–196.
26. Eggleton, R.A.; Fitzpatrick, R.W. New data and a revised structural model for ferrihydrite. *Clays Clay Miner.* **1988**, *36*, 111–124.
27. Châtellier, X.; West, M.M.; Rose, J.; Fortin, D.; Leppard, G.G.; Ferris, F.G. Characterizations of iron-oxides formed by oxidation of ferrous ions in the presence of various bacterial species and inorganic ligands. *Geomicrobiol. J.* **2004**, *21*, 99–112.
28. Karim, Z. Characteristics of ferrihydrites formed by oxidation of $FeCl_2$ solutions containing different amounts of silica. *Clays Clay Minerals* **1984**, *32*, 181–184.
29. Carlson, L.; Schwertmann, U. Natural ferrihydrites in surface deposits from Finland and their association with silica. *Geochim. Cosmochim. Acta* **1981**, *45*, 421–429.
30. Dyer, L.; Fawell, P.D.; Newman, O.M.G.; Richmond, W.R. Synthesis and characterization of ferrihydrite/silica co-precipitates. *J. Colloid Interface Sci.* **2010**, *348*, 65–70.
31. Dyer, L.M.; Chapman, K.W.; English, P.; Saunders, M.; Richmond, W. Insights into the crystal and aggregate structure of Fe^{3+} oxide/silica co-precipitates. *Am. Mineral.* **2012**, *97*, 63–69.
32. Seehra, M.S.; Roy, P.; Raman, A.; Manivannan, A. Structural investigations of synthetic ferrihydrite nanoparticles doped with Si. *Solid State Commun.* **2004**, *130*, 597–601.
33. Toner, B.M.; Santelli, C.M.; Marcus, M.A.; Wirth, R.; Chan, C.S.; McCollon, T.; Bach, W. Biogenic iron oxyhydroxide formation at mid-ocean ridge hydrothermal vents: Juan de Fuca Ridge. *Geochim. Cosmochim. Acta* **2009**, *73*, 388–403.
34. Emerson, D.; Ghiorse, W.C. Ultrastructure and chemical composition of the sheath of *Leptothrix discophora* SP-6. *J. Bacteriol.* **1993**, *175*, 7808–7818.
35. Emerson, D.; Ghiorse, W.C. Role of disulfide bonds in maintaining the structural integrity of the sheath of *Leptothrix discophora* SP-6. *J. Bacteriol.* **1993**, *175*, 7819–7827.

36. Sakai, T.; Miyazaki, Y.; Murakami, A.; Sakamoto, N.; Ema, T.; Hashimoto, H.; Furutani, M.; Nakanishi, M.; Fujii, T.; Takada, J. Chemical modification of biogenous iron oxide to create an excellent enzyme scaffold. *Org. Biomol. Chem.* **2010**, *8*, 336–338.
37. Takeda, M.; Makita, H.; Ohno, K.; Nakahara, Y.; Koizumi, J. Structural analysis of the sheath of a sheathed bacterium, *Leptothrix cholodnii*. *Int. J. Biol. Macromol.* **2005**, *37*, 92–98.
38. Mann, S. *Biomineralization: Principles and Concepts in Biogenic Materials Chemistry*; Oxford University Press: Oxford, UK, 2001; pp. 154–196.
39. Hashimoto, H.; Itadani, A.; Kudoh, T.; Kuroda, Y.; Seno, M.; Kusano, Y.; Ikeda, Y.; Nakanishi, M.; Fujii, T.; Takada, J. Acidic amorphous silica prepared from iron oxide of bacterial origin. *ACS Appl. Mater. Interfaces* **2013**, *5*, 518–523.
40. Hashimoto, H.; Itadani, A.; Fujii, T.; Nakanishi, M.; Asaoka, H.; Kusano, Y.; Ikeda, Y.; Kuroda, Y.; Takada, J. Nano–micro-architectural composites with acid properties: Magnetic iron oxides/amorphous silicate prepared from iron oxide produced by iron-oxidizing bacterium, *Leptothrix ochracea*. *Mater. Res. Bull.* **2013**, *48*, 1174–1177.